Targeting inter-organ cross-talk in cardiometabolic diseases

Liu, C.

2

Choline and butyrate beneficially modulate the gut microbiome without affecting atherosclerosis in *APOE*3-Leiden.CETP* mice

Cong Liu[1,2], Zhuang Li[1,2], Zikuan Song[1,2], Xiayue Fan[3], Hua Shao[3], Milena Schönke[1,2], Mariëtte R. Boon[1,2], Patrick C.N. Rensen[1,2,3], Yanan Wang[1,2,3]

[1] Department of Medicine, Division of Endocrinology, Leiden University Medical Center, Leiden, The Netherlands.
[2] Einthoven Laboratory for Experimental Vascular Medicine, Leiden University Medical Center, Leiden, The Netherlands.
[3] Med-X institute, Center for Immunological and Metabolic Diseases, and Department of Endocrinology, First Affiliated Hospital of Xi'an Jiaotong University, Xi'an Jiaotong University, Xi'an, China.

Atherosclerosis, 2022; 362: 47-55.

ABSTRACT

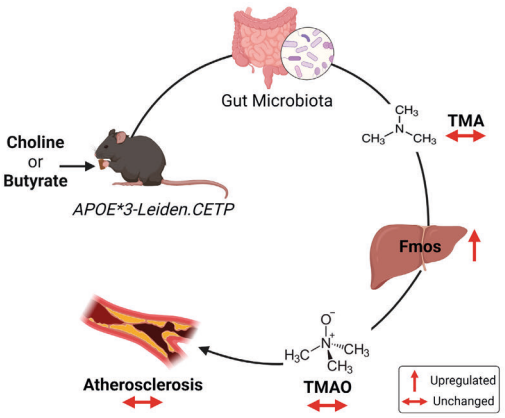

Choline has been shown to exert atherogenic effects in *Apoe*$^{-/-}$ and *Ldlr*$^{-/-}$ mice, related to its conversion by gut bacteria into trimethylamine (TMA) that is converted by the liver into the proinflammatory metabolite trimethylamine-N-oxide (TMAO). Since butyrate beneficially modulates the gut microbiota and has anti-inflammatory and antiatherogenic properties, the aim of the present study was to investigate whether butyrate can alleviate choline-induced atherosclerosis. To this end, we used *APOE*3-Leiden.CETP* mice, a well-established atherosclerosis-prone model with human-like lipoprotein metabolism. Female *APOE*3-Leiden.CETP* mice were fed an atherogenic diet alone or supplemented with choline, butyrate or their combination for 16 weeks. Interestingly, choline protected against fat mass gain, increased the abundance of anti-inflammatory gut microbes, and increased the expression of gut microbial genes involved in TMA and TMAO degradation. Butyrate similarly attenuated fat mass gain and beneficially modulated the gut microbiome, as shown by increased abundance of anti-inflammatory and short chain fatty acid-producing microbes, and inhibited expression of gut microbial genes involved in lipopolysaccharide synthesis. Both choline and butyrate upregulated hepatic expression of flavin-containing monooxygenases, and their combination resulted in highest circulating TMAO levels. Nonetheless, choline, butyrate and their combination did not influence atherosclerosis development, and TMAO levels were not associated with atherosclerotic lesion size. While choline and butyrate have been reported to oppositely modulate atherosclerosis development in *Apoe*$^{-/-}$ and *Ldlr*$^{-/-}$ mice as related to changes in the gut microbiota, both dietary constituents did not affect atherosclerosis development while beneficially modulating the gut microbiome in *APOE*3-Leiden.CETP* mice.

INTRODUCTION

Atherosclerosis, the main underlying cause of cardiovascular diseases (CVD), is a chronic disease arising from an imbalanced cholesterol metabolism and a maladaptive immune response [1]. Hypercholesterolemia induces the retention of apolipoprotein (Apo) B-containing cholesterol-rich lipoproteins in the arterial intima, which triggers infiltration of circulating monocytes into the intima, induces cholesterol-laden foam cell formation and accumulation, and subsequently initiates and aggravates atherosclerosis [1]. Therefore, cholesterol-lowering therapy potently reduces morbidity and mortality of atherosclerotic CVD (asCVD) [2]. Yet, a significant burden of asCVD remains, at least partly due to the residual inflammatory risk [3]. Therefore, there is an urgent need to search for additional therapeutic targets which govern atherogenesis, particularly those regulating both cholesterol metabolism and inflammation.

Several lines of evidence have linked the gut microbiota to atherogenesis [4, 5]. The gut microbiota is mainly shaped by dietary factors. Bacteria in the gut can metabolize complex dietary components to generate various functional small-molecule metabolites [4, 5]. Trimethylamine N-oxide (TMAO) is a gut-derived metabolite that has been described to aggravate atherosclerosis in *Apoe*$^{-/-}$ and *Ldlr*$^{-/-}$ mice [6, 7]. Gut microbiota generate TMAO from dietary choline via a two-step meta-organismal pathway to first produce trimethylamine (TMA) that is delivered via the portal vein to the liver where it can be rapidly oxidized into TMAO by flavin monooxygenases (FMOs). TMAO aggravates atherosclerosis via various mechanisms, such as promoting foam cell formation and activation of the inflammatory response [6, 8]. Hence, TMAO-lowering interventions may have therapeutic potential to reduce asCVD risk. Interestingly, butyrate, a short chain fatty acid (SCFA), has been shown to protect against atherosclerosis in *Apoe*$^{-/-}$ and *Ldlr*$^{-/-}$ mice [9-12]. This is in part mediated through its action on the gut microbiota, since butyrate suppresses the overgrowth of pathogenic gut microbes, inhibits the synthesis of endotoxins, and prevents bacterial translocation. As a result, butyrate alleviates systemic inflammation, thereby halting atherosclerosis progression [9].

Based on the hypothesis that butyrate may be able to protect against dietary choline-induced atherosclerosis development, the aim of the present study was to examine the effects of choline, butyrate and their combination on atherosclerosis in *APOE*3-Leiden.CETP* mice, a well-established translational model for human-like lipoprotein metabolism. In contrast to our expectations, we demonstrate that both choline and butyrate beneficially modulate the gut microbiome without affecting atherosclerosis development, and TMAO levels were not associated with atherosclerotic lesion size.

MATERIALS AND METHODS

For details of animals and antibodies used, please see the Major Resources Table in the **Supplementary Materials**.

Mice

Female *APOE*3-Leiden.CETP* mice were generated as previously described [13]. Mice at the age of 8-12 weeks were housed under standard conditions (22℃; 12/12-hour light/dark cycle) with *ad libitum* access to water and a cholesterol-containing Western-type diet (WTD; 0.15% cholesterol and 16% fat; ssniff, Soest, Germany). All mice were acclimatized to housing and WTD for 3 weeks prior to the dietary intervention. Then, based on 4-hour fasted plasma lipid levels, body weight as well as body composition, these mice were randomized to 4 treatment groups using RandoMice [14] (n=17 per group) receiving either WTD (ctrl group), WTD+choline (1.2% w/w, according to previous studies [6, 15]; choline group), WTD+butyrate (5% w/w, according to previous studies [16, 17]; butyrate group) or WTD+butyrate+choline (1.2% w/w choline and 5% w/w butyrate; butyrate+choline group) for 16 weeks according to a well-established protocol in our group [18-20]. The sample size was calculated based on the average atherosclerotic lesion area of 1×10^5 μm^2 in the ctrl group with a standard deviation lesion size of 0.3×10^5 μm^2. We considered a difference in plaque size of 30% to be biologically relevant. To achieve the differences with α=5% and a power of 80%, 17 animals per group were therefore needed. Mice were group housed (4-5 per cage) during the experimental period to avoid stress caused by single housing. All animal experiments were performed in accordance with the Institute for Laboratory Animal Research Guide for the Care and Use of Laboratory Animals, and were approved by the National Committee for Animal Experiments and by the Ethics Committee on Animal Care (Protocol No. AVD1160020172927) and Experimentation of the Leiden University Medical Center (Protocol No. PE.18.063.006). All animal procedures were conform the guidelines from Directive 2010/63/EU of the European Parliament on the protection of animal used for scientific purposes.

Body weight and body composition

Body weight was measured weekly with a scale, and body composition of conscious mice was measured biweekly using an EchoMRI-100 analyzer (EchoMRI, Houston, TX, USA).

Plasma lipid profiles and choline metabolites

Every 4 weeks, after 4 hours of fasting (9:00-13:00), tail vein blood was collected into paraoxon-coated glass capillaries. These capillaries were placed on ice and centrifuged, and plasma was collected and stored at -20℃. Plasma total cholesterol (TC) and

triglyceride (TG) levels were determined (n=17 per group) using commercial enzymatic kits from Roche Diagnostics (Mannheim, Germany). Plasma high density lipoprotein cholesterol (HDL-C) and non-HDL-C levels (n=17 per group) were determined as previously described [19]. At week 16, plasma choline, betaine, TMA and TMAO levels were quantified (n=10 per group) using liquid chromatography-tandem mass spectrometry as described under Expanded Methods in the **Supplementary Materials**.

Gene expression

Total RNA was extracted from snap-frozen tissues using the Tripure RNA isolation reagent (Roche, Mijdrecht, The Netherlands), according to the manufacturer's instructions. Complementary DNA for quantitative reverse transcriptase-PCR was generated as previously described [18]. The expression of mRNA was normalized to *Actb* and *Rplp0* mRNA levels and expressed as fold change compared with the ctrl group. The primer sequences are listed in the **Supplementary Materials**.

Genomic DNA extraction and metagenomic sequencing

At week 16, cecal contents were collected, and genomic bacterial DNA was isolated with the fast DNA stool mini kit (QIAamp, Germany) following the manufacturer's instructions. Then, these DNA samples were used for determination of gut microbial gene expression via qPCR as well as metagenomics sequencing. Sequencing data was processed as described under Expanded Methods in the **Supplementary Materials**.

Atherosclerotic plaque characterization and quantification

Hearts were collected and fixated in phosphate-buffered 4% formaldehyde, embedded in paraffin after dehydration in 70-100% ethanol and cross-sectioned (5 μm) perpendicular to the axis of the aorta throughout the aortic root area, starting from the appearance of open aortic valve leaflets. Per mouse, 4 sections with 50 μm intervals were used for atherosclerosis measurements. Sections were stained with haematoxylin-phloxine-saffron for histological analysis. Lesions were categorized by severity according to the guidelines of the American Heart Association adapted for mice [21]. Sirius Red staining was used to quantify the collagen area. Monoclonal mouse antibody M0851 (1:800; Dako, Heverlee, The Netherlands) against smooth muscle cell actin was used to quantify the smooth muscle cell area. Rat monoclonal anti-mouse MAC-3 antibody (1:1000; BD Pharmingen, San Diego, CA, USA) was used to quantify the macrophage area. Immunostainings were amplified using Vector Laboratories Elite ABC kit (Vector Laboratories Inc., Burlingame, CA, USA) and the immune-peroxidase complex was visualized with Nova Red (Vector Laboratories Inc., Burlingame, CA, USA). Lesion area and composition were analyzed using Image J software. The stability index was calculated by dividing the relative collagen and smooth muscle cell area by the relative area of macrophages within the same lesion.

Statistical analyses

Statistical analyses among these 4 groups were assessed using One-way ANOVA followed by a Fisher's LSD post hoc test, unless indicated otherwise. The square root of the lesion area was taken to linearize the relationship with the plasma TC, non-HDL-C, HDL-C and TG exposures and plasma TMAO levels (at 16 week). To assess significant correlations between atherosclerotic lesion size and plasma lipids and TMAO, univariate regression analyses were performed. Then, to predict the contribution of these plasma parameters to the atherosclerotic lesion size, multiple regression analysis was performed. Data are presented as mean±SEM, and a *P* value less than 0.05 is considered statistically significant. All statistical analyses were performed with GraphPad Prism 9 (GraphPad Software Inc., California, CA, USA) except for univariate and multiple regression analyses which were performed with SPSS 20.0 (SPSS, Chicago, IL USA) for Windows and metagenomic data analysis using R packages.

RESULTS

Choline and butyrate attenuate WTD-induced fat mass gain in *APOE*3-Leiden.CETP* mice

To address how choline and butyrate affect atherosclerosis in a mouse model for human-like lipoprotein metabolism, we fed female *APOE*3-Leiden.CETP* mice a cholesterol-containing WTD alone or supplemented with choline, butyrate or a combination of

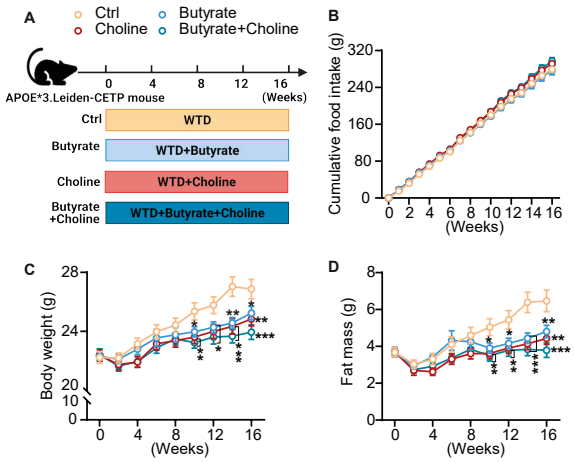

Fig. 1. Choline and butyrate attenuate WTD-induced fat mass gain in *APOE*3-Leiden.CETP* mice. (**A**) Experimental set up. (**B**) Cumulative food intake (n=4-5 per group), (**C**) body weight (n=16-17 per group), and (**D**) body fat mass (n=16-17 per group) were monitored throughout the experimental period. Data are shown as mean±SEM. Differences were assessed using one-way ANOVA followed by a Fisher's LSD post-test. **P*<0.05; ***P*<0.01, ****P*<0.001, compared with the control (ctrl) group. WTD, Western-type diet.

both supplements for 16 weeks (**Fig. 1A**). Neither choline nor butyrate affected food intake (**Fig. 1B**). Despite this, choline and butyrate attenuated WTD-induced body weight gain (**Fig. 1C**), which was explained by reduced fat mass gain (**Fig. 1D**) without affecting body lean mass (**Fig. S1**).

Choline and butyrate beneficially modulate the gut microbiome in *APOE*3-Leiden.CETP* mice

Previous studies have shown that the gut microbiota participates in choline- and butyrate-induced modulation of body weight and atherogenesis [16, 22, 23]. We thus performed whole metagenome shotgun sequencing to assess the impact of choline, butyrate and their combination on the gut microbiota composition and function. While principal component analysis revealed great similarities of the gut microbiome structure among the groups (**Fig. 2A**), choline reduced the gut microbial α diversity, regardless of butyrate supplementation (**Fig. 2B**). At the phylum level, most gut commensal microbes belonged to *Bacteroidetes*, *Firmicutes*, *Proteobacteria*, which, along with *Actinobacteria* and *Verrucomicrobia*, represented approximately 95% of the total microbial community (**Fig. S2A**). At the species level, *Faecalibaculum rodentium* (*F. rodentium*), *Parabacteroides distasonis* (*P. distasonis*) and *Bacteroides uniforms* (*B. uniforms*) were abundant among the groups (**Fig. 2C**). As compared to control treatment, butyrate enriched species with proposed anti-inflammatory properties, such as *Duncaniella spB8* (*D. spB8*) [24, 25] and *Blautia producta* (*B. producta*) [26], *Faecalibaculum* (*F. prausnitzii*) [27, 28] and *Ruthenibacterium lactatiformans* (*R. lactatiformans*) [29] (**Fig. 2D**).

Simultaneously, butyrate downregulated gut microbial genes involved in lipopolysaccharide (LPS) biosynthesis when compared to control treatment (**Fig. 2E**, **S2B**). In addition, choline increased several bacterial species compared to control treatment, including a probiotic microbe *Lactobacillus reuteria* (*L. reuteria*) [30] and three anti-inflammatory species of the *Olsenella* genus [31] (**Fig. 2F**). Interestingly, choline treatment did not affect TMA-producing bacteria, had no impact on gut microbial genes associated with TMA synthesis (**Fig. 2G**), and did not affect the expression of choline trimethylamine-lyase (*CutC*), an essential bacterial choline TMA-lyase gene (**Fig. 2H**). Rather, choline treatment upregulated gene expression of enzymes involved in TMA and TMAO degradation, including TMA corrinoid protein and TMAO reductase (**Fig. 2I**), effects that were blunted upon concomitant butyrate administration (**Fig. S2C-E**). Moreover, choline treatment upregulated gut microbial genes involved in starch and sugar metabolism (**Fig. 2G**), which are associated with SCFA production [32]. Furthermore, the combination group shared greater similarities in the gut composition and function compared to the choline group than the butyrate

group (**Fig. S3A-E**). Taken together, both choline and butyrate beneficially affected the gut microbial composition and function in WTD-fed *APOE*3-Leiden-CETP* mice, with a greater impact on the gut microbiome induced by choline versus butyrate.

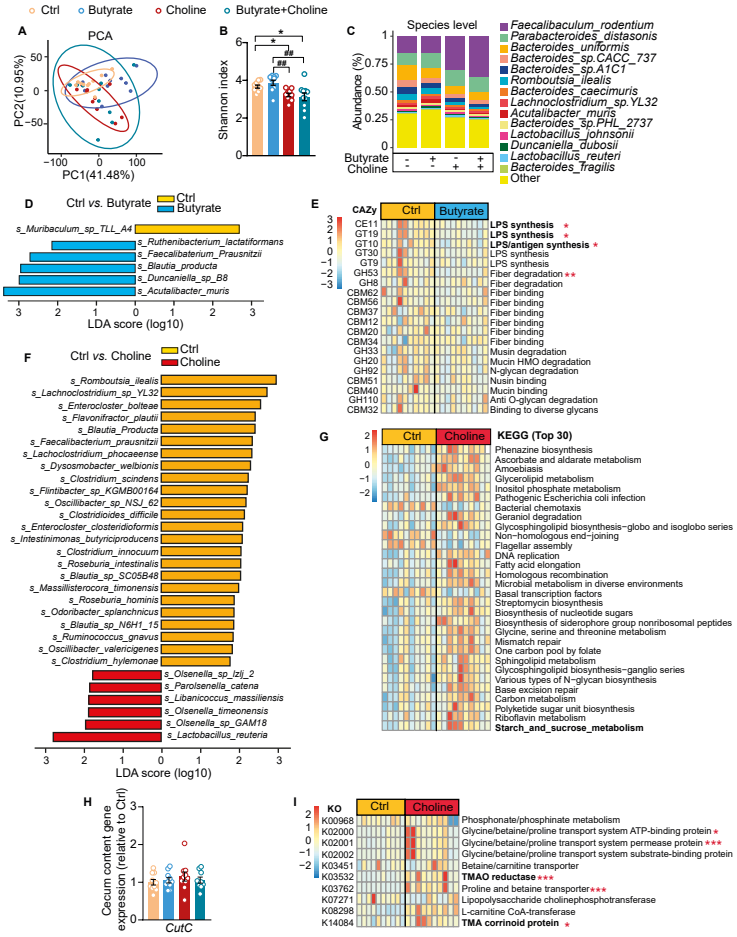

Fig. 2. Choline and butyrate beneficially modulate the gut microbiome in *APOE*3-Leiden.CETP* mice. At the end of the study, the cecal content was collected and sequenced using metagenomics sequencing (n=10 per group). (**A**) Principal component analysis (PCA) at the species level. (**B**) The Shannon index at the species level. (**C**) The abundance of the top 15 microbial species. (**D** and **F**) Linear discrimination analysis (LDA) effect size analysis was performed, and LDA scores calculated for differences in species-level abundance between groups. (**E** and **I**) Relative changes of the gut microbial genes involved in lipopolysaccharide (LPS) signaling and the metabolic pathway of TMA. (**G**) Top 30 significantly regulated KEGG pathways between the ctrl and choline groups. (**H**) Relative gut microbial *CutC* (choline TMA lyase) expression. (**B**, **H**) Data are represented as means±SEM. Differences were assessed using one-way ANOVA followed by a Fisher's LSD post-test. (**E**, **G**, **I**) Comparisons between groups were performed using Wilcoxon test. **P*<0.05; ***P*<0.01, ****P*<0.001, compared with the ctrl group. $^{\#\#}$*P*<0.01, compared to the butyrate group.

Co-administration of choline and butyrate, instead of choline or butyrate alone, increases plasma TMAO levels in *APOE*3-Leiden.CETP* mice

Then, we investigated the role of dietary choline and butyrate in choline metabolism. To this end, we performed targeted metabolomics analyses to measure choline-related metabolites in plasma. Dietary choline increased plasma levels of choline and its oxidation product betaine (**Fig. 3A-B**) without affecting plasma TMA levels (**Fig. 3C**), while butyrate did not alter the levels of choline and its metabolites (**Fig. 3A-D**). Of note, only combination treatment increased TMAO levels (**Fig. 3D**). We observed that both choline and butyrate upregulated the hepatic expression of *Fmos* (i.e., *Fmo2* and *Fmo3*; **Fig. 3E**). Co-administration of choline and butyrate caused the highest expression of *Fmo3* in the liver (**Fig. 3E**), which may explain the highest plasma TMAO levels in the combination group.

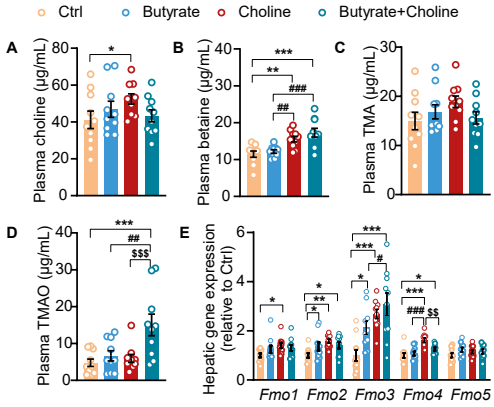

Fig. 3. Co-administration of choline and butyrate, instead of choline or butyrate alone, increases plasma TMAO levels in *APOE*3-Leiden.CETP* mice. At week16, plasma levels of **(A)** choline, (**B**) betaine, (**C**) TMA and (**D**) TMAO were determined. (**E**) At the end of the study, the relative mRNA expression of flavin-containing monooxygenases (*Fmos*) was determined in the liver. Data are shown as mean±SEM (n=10 per group). Differences were assessed using one-way ANOVA followed by a Fisher's LSD post hoc test. $^{*}P<0.05$; $^{**}P<0.01$, $^{***}P<0.001$, compared with the ctrl group; $^{\#}P<0.05$, $^{\#\#}P<0.01$, $^{\#\#\#}P<0.001$, compared to the butyrate group; $^{\$\$}P<0.01$, $^{\$\$\$}P<0.001$, compared to the choline group. *Fmos*, flavin monooxygenases; TMA, trimethylamine; TMAO, trimethylamine N-oxide.

Choline and butyrate do not affect plasma lipid levels in *APOE*3-Leiden.CETP* mice

Choline and butyrate have been suggested to modulate reverse cholesterol transport (RCT) [11, 33]. However, choline upregulated to only some extent the expression of genes involved in HDL assembly (e.g. ATP-binding cassette subfamily A member 1, *Abca1*; **Fig. 4A**;), HDL uptake (e.g. scavenger receptor class B type 1, *Srb-1*; **Fig. 4B**),

bile acid secretion (e.g. bile salt export pump, *Bsep*; **Fig. 4C**), sterol secretion (e.g. ATP-binding cassette transporter G member 5, *Abcg5*; **Fig. 4D**), *Ldlr* and *CETP* (**Fig. 4E**). And, butyrate had minor impact on the expression of these genes (**Fig. 4A-E**). Similarly, neither choline nor butyrate had any evident effects on levels of plasma TG, TC, HDL-C and non-HDL-C (**Fig. S4A-B**, **4F-G**).

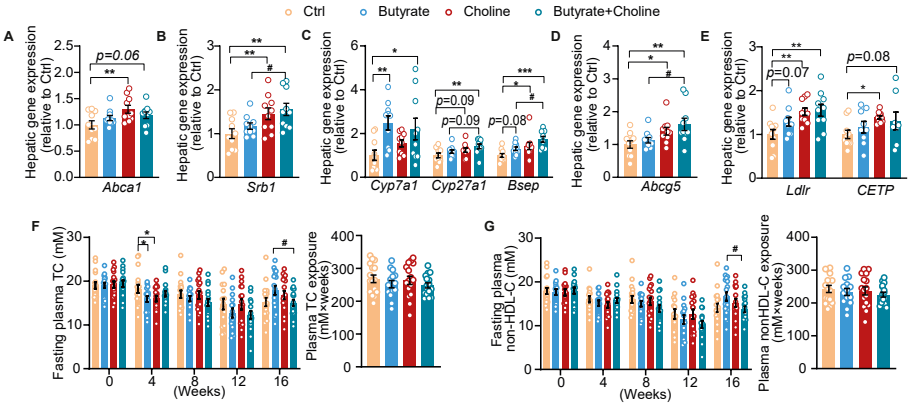

Fig. 4. Choline and butyrate do not affect plasma lipid levels in *APOE*3-Leiden.CETP* mice. The relative expression of genes involved in high-density lipoprotein (HDL) assembly and clearance (**A** and **B**), bile acid synthesis and secretion (**C**), and sterol secretion (**D**) was determined. (**E**) The mRNA levels of low-density lipoprotein receptor and cholesteryl ester transfer protein (*CETP*) were measured. Fasting plasma levels of total cholesterol (TC; **F)** and non-high-density lipoprotein cholesterol (non-HDL-C; **G**) were determined throughout the experimental period. Data are represented as mean±SEM (**A-E**, n=9-10 per group; **F-G**, n=16-17 per group). Differences were assessed using one-way ANOVA followed by a Fisher's LSD post hoc test. **P*<0.05; ***P*<0.01, ****P*<0.001, compared with the ctrl group; #*P*<0.05, compared to the butyrate group. *Abca1*, ATP-binding cassette subfamily A member 1; *Abcg5*, ATP-binding cassette transporter G member 5; *Bsep*, bile salt export pump; *Cyp27a1*, sterol 27-hydroxylase; *Cyp7a1*, cholesterol 7α-hydroxylase; *Ldlr*, low density lipoprotein receptor; *Srb-1*, scavenger receptor class B type 1.

Choline and butyrate have no impact on atherosclerosis development in *APOE*3-Leiden-CETP* mice

We next assessed the size, severity and composition of atherosclerotic lesions throughout the aortic root in the heart isolated after 16 weeks of treatment. Neither choline, butyrate nor their combination affected atherosclerotic plaque area, severity and composition (**Fig. 5A-D, S5A-C**). In accordance, choline and butyrate had no impact on atherosclerotic plaque stability (**Fig. 5E**), as calculated from dividing the relative collagen and smooth muscle cell area by the relative area of macrophages within the same lesion. While univariate regression analysis revealed that the atherosclerotic lesion area was to some extent predicted by plasma cholesterol levels (**Fig. 5F**, **S5D-F**), plasma TMAO levels were not associated with atherosclerotic lesion size in *APOE*3.Leiden-CETP* mice (**Fig. 5G**).

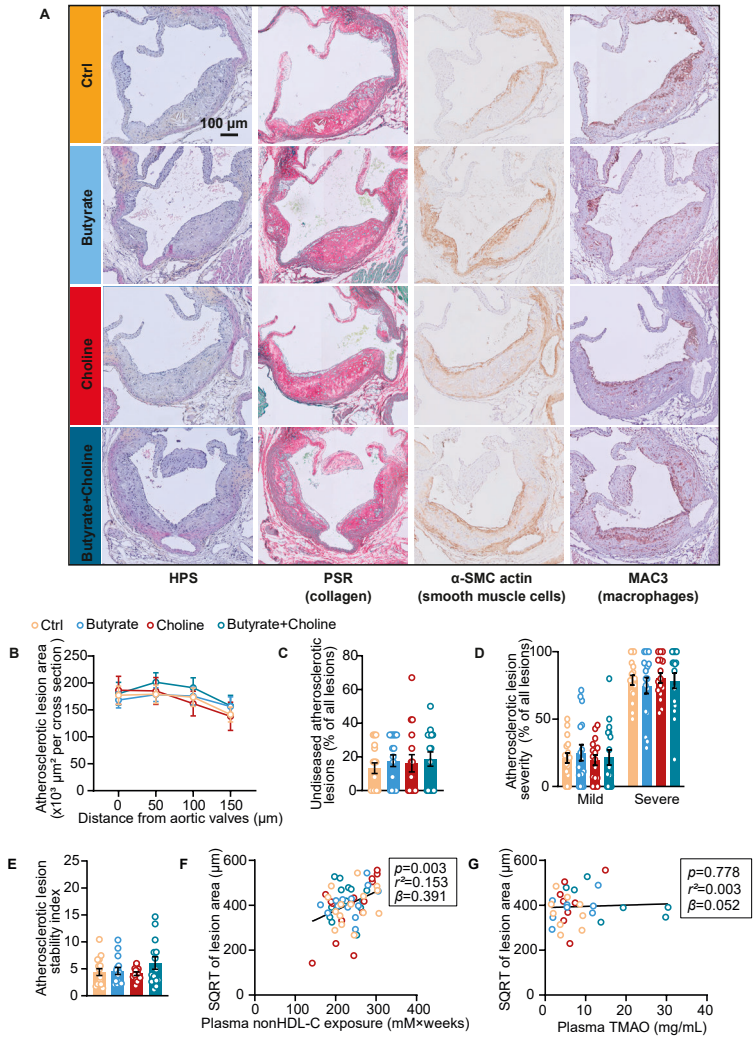

Fig. 5. Choline and butyrate have no impact on atherosclerosis development in *APOE*3-Leiden.CETP* mice. At 16 weeks, hearts were collected, and the valve area in the aortic root was stained with haematoxylin–phloxine–saffron (HPS). To quantify the contents of collagen, smooth muscle cells and macrophages within the lesion, the valve area in the aortic root was stained with Picrosirius red (PSR), anti-α-smooth muscle cell actin (α-SMC actin) antibody and anti-MAC3 antibody, respectively. (**A**) Representative pictures of every staining. (**B**) The relationship between atherosclerotic lesion area and the distance from aortic valve was determined by calculating the lesion area of 4 consecutive sections (with 50 µm intervals) beginning with the appearance of open aortic valve leaflets (n=13-16 per group). Lesions were categorized into undiseased (**C**), mild, and severe (**D**) lesions (n=13-16 per group). (**E**) The stability index was calculated by dividing the smooth muscle cell and collagen area by macrophage area within the same lesion. The square root (SQRT) of the atherosclerotic lesion area plotted against plasma (**F**) non-HDL-C exposure and TMAO (**G**) levels, and linear regression analyses were performed. Data are represented as means±SEM (**B-F**, n=13-16 per group; **G**, n=10 per group). Comparisons among four groups were performed using one-way ANOVA followed by a Fisher's LSD post hoc test.

DISCUSSION

Choline has been reported to aggravate atherosclerosis development, as caused by generation of TMAO through the gut-liver axis [6, 33], while butyrate beneficially modulates the gut microbiota and shows antiatherogenic effects, in *Apoe*$^{-/-}$ and *Ldlr*$^{-/-}$ mice [9-11]. Based on our hypothesis that butyrate is able to alleviate choline-induced atherosclerosis, we set out to evaluate the effects of choline, butyrate and their combination in *APOE*3.Leiden-CETP* mice, a well-established model for human-like lipid metabolism and atherosclerosis development. In contrast to expectations, we here report that both choline and butyrate beneficially modulate the gut microbiome, without affecting atherosclerosis development. Likewise, the combination of choline and butyrate did not influence atherosclerosis development, and TMAO levels were not associated with atherosclerotic lesion size.

First, we demonstrated that choline exerts beneficial effects on the gut microbial composition and function without influencing atherosclerosis. Choline increased cecal abundance of *L. reuteria* and three species in the *Olsenella* genus. *L. reuteria* has been reported to improve gut barrier function via reducing inflammation [30, 34], and bacteria of the *Olsenella* genus enhance the efficacy of immune checkpoint inhibitors in cancer by enhancing anti-inflammatory capacities of T cells [31]. In this study, choline did not affect the cecum content expression of bacterial *CutC*, a key gene responsible for converting choline into TMA by the gut microbiota. In line with this finding, choline did not affect plasma TMA levels. Choline did upregulate hepatic expression of *Fmos* (especially *Fmo3*), encoding the rate-limiting enzymes responsible for the oxidation of TMA to TMAO [15, 33]. However, choline did not influence plasma TMAO levels, which may be explained by upregulated gut microbial gene expression of TMAO reductase that reduces TMAO to TMA, and TMA corrinoid that catabolizes TMA to methane [35, 36]. It has been shown that excess choline can also be metabolized to other metabolites, such as phosphocholine and acetylcholine [37-39], and the mouse model used here may have different choline metabolism compared to other mouse models such as *Apoe*$^{-/-}$ and *Ldlr*$^{-/-}$ mice. Thus, future studies are needed to explore the differences in choline metabolism between in the various mouse models. In addition, we observed that choline slightly upregulated hepatic expression of RCT-related genes. This is in contrast to previous studies in *Apoe*$^{-/-}$ mice, which proposed that choline suppresses expression of RCT-related genes to aggravate atherosclerosis [33], although it is in fact in line with the absence of effects of choline on atherosclerosis in *APOE*3-Leiden.CETP* mice. We did observe that choline profoundly upregulates hepatic expression of *CETP* and *Ldlr*. Therefore, the seeming discrepancies between the different mouse models might be explained by a choline-mediated increase of CETP-mediated transfer

of neutral lipids between lipoproteins and a APOE-LDLR mediated clearance pathway of triglyceride-rich lipoprotein remnants, which are both operational in *APOE*3-Leiden.CETP* mice but not in *ApoE*$^{-/-}$ mice. In fact, and in line with our findings, a very recent study showed that choline does not affect atherosclerosis in CETP-expressing *Apoe*$^{-/-}$ mice [40].

Similarly to choline, butyrate also beneficially modulated the gut microbiome although in different aspects. Butyrate increased cecal abundance of the anti-inflammatory species *D. spB8* [24, 25] as well as three strains known for producing SCFAs, including acetate-producing *B. producta* [26], butyrate-producing *F. Prausnitzii* [27, 28] and lactate-producing *R. lactatiformans* [29]. Furthermore, butyrate downregulated cecal microbial genes involved in LPS synthesis, which may imply that butyrate alleviates LPS-induced damage of gut barrier integrity [41]. Previous studies showed that butyrate reduces atherosclerotic lesion size in *Apoe*$^{-/-}$ and *Ldlr*$^{-/-}$ mice partially via improving gut barrier function [9-12, 42]. This was attributed to maintained gut microbiota homeostasis and inhibited LPS synthesis, which reduces gut barrier permeability and thus reduces systemic inflammation [42-44]. Probably as a combined result, butyrate inhibited macrophage infiltration into atherosclerotic plaques and halts plaque progression [9, 45]. In contrast, we found no influence of butyrate on atherosclerotic size, severity and composition including macrophage content within atherosclerotic lesions in *APOE*3-Leiden.CETP* mice. In addition to beneficially modulating gut microbiome, butyrate has been demonstrated to promote RCT and thus to improve cholesterol metabolism, by primarily stimulating ABCA1-mediated cholesterol efflux in macrophages and increasing hepatic bile acid synthesis and secretion, thereby alleviating atherosclerosis in *Apoe*$^{-/-}$ mice [11]. In our mouse model, butyrate only slightly affected hepatic expression of RCT-related genes including *Abca1* and did not affect cholesterol levels. Moreover, plasma non-HDL-C levels were positively correlated to atherosclerotic size. Therefore, it is likely that atherosclerosis is more inflammation-driven in *Apoe*$^{-/-}$ and *Ldlr*$^{-/-}$ mice, and more cholesterol-driven in *APOE*3-Leiden.CETP* mice, explaining why butyrate is not atheroprotective in our model.

TMAO has been identified as the main mediator of the previously described atherogenic effects of choline in *Apoe*$^{-/-}$ and *Ldlr*$^{-/-}$ mice [6, 33]. In the present study, we observed that treatment with the combination of choline and butyrate increased plasma TMAO levels as compared to single treatments. This is likely due to the observation that butyrate impaired the choline-induced TMA and TMAO degradation signaling. Indeed, the gut microbial gene expression of TMA corrinoid protein and TMAO reductase in the combination group was comparable to that of the control and butyrate groups. However, in spite of increased plasma TMAO levels, combined choline and butyrate

administration did not affect atherosclerosis. Of note, plasma TMAO levels were not associated with atherosclerotic lesion size. The fact that TMAO induces atherosclerosis in *Apoe*$^{-/-}$ and *Ldlr*$^{-/-}$ mice but not in *APOE*3-Leiden.CETP* mice, may suggest that TMAO lacks atherogenic properties in humans. Indeed, many human dietary trials did not find any association between plasma TMAO and CVD risk [46-48]. Multiple meta-analyses and systematic reviews have shown that the intake of eggs, rich in TMAO precursors, is not correlated to heart disease risk and mortality [49]. Similarly, another systematic review and a cohort study have concluded that TMAO does not associate with CVD risk [50].

In conclusion, we demonstrate that in *APOE*3-Leiden.CETP* mice, a well-established model for human-like lipoprotein metabolism, both choline and butyrate beneficially modulate the gut microbiome and increase TMAO, however without affecting atherosclerosis.

Acknowledgments

We thank T.C.M. Streefland, A.C.M. Pronk, R.A. Lalai and S. Afkir from the Department of Medicine, Division of Endocrinology, Leiden University Medical Center for technical assistance.

Author contributions

CL designed the study, carried out the research, analyzed and interpreted the results, and wrote and revised the manuscript. ZL carried out the research, interpreted the results, reviewed and revised the manuscript, and obtained funding. ZS carried out the research, interpreted the results, reviewed and revised the manuscript. XF and HS analyzed metagenomics data and reviewed the manuscript. MS interpreted the results, reviewed and revised the manuscript. MRB advised the study and reviewed the manuscript. PCNR designed and advised the study, interpreted the results, edited, reviewed and revised the manuscript and obtained funding. YW designed and advised the study, interpreted the results, reviewed and revised the manuscript and obtained the funding.

REFERENCES

1. Back M, Yurdagul A, Jr., Tabas I, Oorni K, Kovanen PT. Inflammation and its resolution in atherosclerosis: mediators and therapeutic opportunities. *Nat Rev Cardiol.* 2019;16:389-406. doi: 10.1038/s41569-019-0169-2
2. Hegele RA, Gidding SS, Ginsberg HN, McPherson R, Raal FJ, Rader DJ, Robinson JG, Welty FK. Nonstatin Low-Density Lipoprotein-Lowering Therapy and Cardiovascular Risk Reduction-Statement From ATVB Council. *Arterioscler Thromb Vasc Biol.* 2015;35:2269-2280. doi: 10.1161/ATVBAHA.115.306442
3. Aday AW, Ridker PM. Targeting Residual Inflammatory Risk: A Shifting Paradigm for Atherosclerotic Disease. *Front Cardiovasc Med.* 2019;6:16. doi: 10.3389/fcvm.2019.00016
4. Jonsson AL, Backhed F. Role of gut microbiota in atherosclerosis. *Nat Rev Cardiol.* 2017;14:79-87. doi: 10.1038/nrcardio.2016.183
5. Tang WHW, Li DY, Hazen SL. Dietary metabolism, the gut microbiome, and heart failure. *Nat Rev Cardiol.* 2019;16:137-154. doi: 10.1038/s41569-018-0108-7
6. Wang Z, Klipfell E, Bennett BJ, Koeth R, Levison BS, Dugar B, Feldstein AE, Britt EB, Fu X, Chung YM, et al. Gut flora metabolism of phosphatidylcholine promotes cardiovascular disease. *Nature.* 2011;472:57-63. doi: 10.1038/nature09922
7. Seldin MM, Meng Y, Qi H, Zhu W, Wang Z, Hazen SL, Lusis AJ, Shih DM. Trimethylamine N-Oxide Promotes Vascular Inflammation Through Signaling of Mitogen-Activated Protein Kinase and Nuclear Factor-kappaB. *J Am Heart Assoc.* 2016;5. doi: 10.1161/JAHA.115.002767
8. Collins HL, Drazul-Schrader D, Sulpizio AC, Koster PD, Williamson Y, Adelman SJ, Owen K, Sanli T, Bellamine A. L-Carnitine intake and high trimethylamine N-oxide plasma levels correlate with low aortic lesions in ApoE(-/-) transgenic mice expressing CETP. *Atherosclerosis.* 2016;244:29-37. doi: 10.1016/j.atherosclerosis.2015.10.108
9. Kasahara K, Krautkramer KA, Org E, Romano KA, Kerby RL, Vivas EI, Mehrabian M, Denu JM, Backheds F, Lusis A, et al. Interactions between Roseburia intestinalis and diet modulate atherogenesis in a murine model. *Nat Microbiol.* 2018;3:1461-1471. doi: 10.1038/s41564-018-0272-x
10. Chen Y, Xu C, Huang R, Song J, Li D, Xia M. Butyrate from pectin fermentation inhibits intestinal cholesterol absorption and attenuates atherosclerosis in apolipoprotein E-deficient mice. *J Nutr Biochem.* 2018;56:175-182. doi: 10.1016/j.jnutbio.2018.02.011
11. Du Y, Li X, Su C, Xi M, Zhang X, Jiang Z, Wang L, Hong B. Butyrate protects against high-fat diet-induced atherosclerosis via up-regulating ABCA1 expression in apolipoprotein E-deficiency mice. *Br J Pharmacol.* 2020;177:1754-1772. doi: 10.1111/bph.14933
12. Brandsma E, Kloosterhuis NJ, Koster M, Dekker DC, Gijbels MJJ, van der Velden S, Rios-Morales M, van Faassen MJR, Loreti MG, de Bruin A, et al. A Proinflammatory Gut Microbiota Increases Systemic Inflammation and Accelerates Atherosclerosis. *Circ Res.* 2019;124:94-100. doi: 10.1161/CIRCRESAHA.118.313234
13. Westerterp M, van der Hoogt CC, de Haan W, Offerman EH, Dallinga-Thie GM, Jukema JW, Havekes LM, Rensen PC. Cholesteryl ester transfer protein decreases high-density lipoprotein and severely aggravates atherosclerosis in APOE*3-Leiden mice. *Arterioscler Thromb Vasc Biol.* 2006;26:2552-2559. doi: 10.1161/01.ATV.0000243925.65265.3c

14. van Eenige R, Verhave PS, Koemans PJ, Tiebosch I, Rensen PCN, Kooijman S. RandoMice, a novel, user-friendly randomization tool in animal research. *PLoS One.* 2020;15:e0237096. doi: 10.1371/journal.pone.0237096

15. Tang WH, Wang Z, Levison BS, Koeth RA, Britt EB, Fu X, Wu Y, Hazen SL. Intestinal microbial metabolism of phosphatidylcholine and cardiovascular risk. *N Engl J Med.* 2013;368:1575-1584. doi: 10.1056/NEJMoa1109400

16. Li Z, Yi CX, Katiraei S, Kooijman S, Zhou E, Chung CK, Gao Y, van den Heuvel JK, Meijer OC, Berbee JFP, et al. Butyrate reduces appetite and activates brown adipose tissue via the gut-brain neural circuit. *Gut.* 2018;67:1269-1279. doi: 10.1136/gutjnl-2017-314050

17. Gao Z, Yin J, Zhang J, Ward RE, Martin RJ, Lefevre M, Cefalu WT, Ye J. Butyrate improves insulin sensitivity and increases energy expenditure in mice. *Diabetes.* 2009;58:1509-1517. doi: 10.2337/db08-1637

18. Liu C, Schonke M, Zhou E, Li Z, Kooijman S, Boon MR, Larsson M, Wallenius K, Dekker N, Barlind L, et al. Pharmacological treatment with FGF21 strongly improves plasma cholesterol metabolism to reduce atherosclerosis. *Cardiovasc Res.* 2022;118:489-502. doi: 10.1093/cvr/cvab076

19. Berbee JF, Boon MR, Khedoe PP, Bartelt A, Schlein C, Worthmann A, Kooijman S, Hoeke G, Mol IM, John C, et al. Brown fat activation reduces hypercholesterolaemia and protects from atherosclerosis development. *Nat Commun.* 2015;6:6356. doi: 10.1038/ncomms7356

20. In Het Panhuis W, Kooijman S, Brouwers B, Verhoeven A, Pronk ACM, Streefland TCM, Giera M, Schrauwen P, Rensen PCN, Schonke M. Mild Exercise Does Not Prevent Atherosclerosis in APOE*3-Leiden.CETP Mice or Improve Lipoprotein Profile of Men with Obesity. *Obesity (Silver Spring).* 2020;28 Suppl 1:S93-S103. doi: 10.1002/oby.22799

21. Wong MC, van Diepen JA, Hu L, Guigas B, de Boer HC, van Puijvelde GH, Kuiper J, van Zonneveld AJ, Shoelson SE, Voshol PJ, et al. Hepatocyte-specific IKKbeta expression aggravates atherosclerosis development in APOE*3-Leiden mice. *Atherosclerosis.* 2012;220:362-368. doi: 10.1016/j.atherosclerosis.2011.06.055

22. Agus A, Clement K, Sokol H. Gut microbiota-derived metabolites as central regulators in metabolic disorders. *Gut.* 2021;70:1174-1182. doi: 10.1136/gutjnl-2020-323071

23. Schugar RC, Gliniak CM, Osborn LJ, Massey W, Sangwan N, Horak A, Banerjee R, Orabi D, Helsley RN, Brown AL, et al. Gut microbe-targeted choline trimethylamine lyase inhibition improves obesity via rewiring of host circadian rhythms. *Elife.* 2022;11. doi: 10.7554/eLife.63998

24. Forster SC, Clare S, Beresford-Jones BS, Harcourt K, Notley G, Stares MD, Kumar N, Soderholm AT, Adoum A, Wong H, et al. Identification of gut microbial species linked with disease variability in a widely used mouse model of colitis. *Nat Microbiol.* 2022;7:590-599. doi: 10.1038/s41564-022-01094-z

25. Feng P, Li Q, Liu L, Wang S, Wu Z, Tao Y, Huang P, Wang P. Crocetin Prolongs Recovery Period of DSS-Induced Colitis via Altering Intestinal Microbiome and Increasing Intestinal Permeability. *Int J Mol Sci.* 2022;23. doi: 10.3390/ijms23073832

26. Aoki R, Onuki M, Hattori K, Ito M, Yamada T, Kamikado K, Kim YG, Nakamoto N, Kimura I, Clarke JM, et al. Commensal microbe-derived acetate suppresses NAFLD/NASH development via hepatic FFAR2 signalling in mice. *Microbiome.* 2021;9:188. doi: 10.1186/s40168-021-01125-7

27. Machiels K, Joossens M, Sabino J, De Preter V, Arijs I, Eeckhaut V, Ballet V, Claes K, Van Immerseel F, Verbeke K, et al. A decrease of the butyrate-producing species Roseburia hominis and Faecalibacterium prausnitzii defines dysbiosis in patients with ulcerative colitis. *Gut.* 2014;63:1275-1283. doi: 10.1136/gutjnl-2013-304833

28. Olsson LM, Boulund F, Nilsson S, Khan MT, Gummesson A, Fagerberg L, Engstrand L, Perkins R, Uhlen M, Bergstrom G, et al. Dynamics of the normal gut microbiota: A longitudinal one-year population study in Sweden. *Cell Host Microbe*. 2022;30:726-739 e723. doi: 10.1016/j.chom.2022.03.002

29. Shkoporov AN, Chaplin AV, Shcherbakova VA, Suzina NE, Kafarskaia LI, Bozhenko VK, Efimov BA. Ruthenibacterium lactatiformans gen. nov., sp. nov., an anaerobic, lactate-producing member of the family Ruminococcaceae isolated from human faeces. *Int J Syst Evol Microbiol*. 2016;66:3041-3049. doi: 10.1099/ijsem.0.001143

30. Zhou Q, Wu F, Chen S, Cen P, Yang Q, Guan J, Cen L, Zhang T, Zhu H, Chen Z. Lactobacillus reuteri improves function of the intestinal barrier in rats with acute liver failure through Nrf-2/HO-1 pathway. *Nutrition*. 2022;99-100:111673. doi: 10.1016/j.nut.2022.111673

31. Mager LF, Burkhard R, Pett N, Cooke NCA, Brown K, Ramay H, Paik S, Stagg J, Groves RA, Gallo M, et al. Microbiome-derived inosine modulates response to checkpoint inhibitor immunotherapy. *Science*. 2020;369:1481-1489. doi: 10.1126/science.abc3421

32. Arpaia N, Campbell C, Fan X, Dikiy S, van der Veeken J, deRoos P, Liu H, Cross JR, Pfeffer K, Coffer PJ, et al. Metabolites produced by commensal bacteria promote peripheral regulatory T-cell generation. *Nature*. 2013;504:451-455. doi: 10.1038/nature12726

33. Koeth RA, Wang Z, Levison BS, Buffa JA, Org E, Sheehy BT, Britt EB, Fu X, Wu Y, Li L, et al. Intestinal microbiota metabolism of L-carnitine, a nutrient in red meat, promotes atherosclerosis. *Nat Med*. 2013;19:576-585. doi: 10.1038/nm.3145

34. Wu H, Xie S, Miao J, Li Y, Wang Z, Wang M, Yu Q. Lactobacillus reuteri maintains intestinal epithelial regeneration and repairs damaged intestinal mucosa. *Gut Microbes*. 2020;11:997-1014. doi: 10.1080/19490976.2020.1734423

35. Ferguson DJ, Jr., Krzycki JA. Reconstitution of trimethylamine-dependent coenzyme M methylation with the trimethylamine corrinoid protein and the isozymes of methyltransferase II from Methanosarcina barkeri. *J Bacteriol*. 1997;179:846-852. doi: 10.1128/jb.179.3.846-852.1997

36. Ellenbogen JB, Jiang R, Kountz DJ, Zhang L, Krzycki JA. The MttB superfamily member MtyB from the human gut symbiont Eubacterium limosum is a cobalamin-dependent gamma-butyrobetaine methyltransferase. *J Biol Chem*. 2021;297:101327. doi: 10.1016/j.jbc.2021.101327

37. Corbin KD, Zeisel SH. Choline metabolism provides novel insights into nonalcoholic fatty liver disease and its progression. *Curr Opin Gastroen*. 2012;28:159-165. doi: 10.1097/MOG.0b013e32834e7b4b

38. Zeisel SH. Metabolic crosstalk between choline/1-carbon metabolism and energy homeostasis. *Clin Chem Lab Med*. 2013;51:467-475. doi: 10.1515/cclm-2012-0518

39. Garcia-Molina P, Sola-Leyva A, Luque-Navarro PM, Laso A, Rios-Marco P, Rios A, Lanari D, Torretta A, Parisini E, Lopez-Cara LC, et al. Anticancer Activity of the Choline Kinase Inhibitor PL48 Is Due to Selective Disruption of Choline Metabolism and Transport Systems in Cancer Cell Lines. *Pharmaceutics*. 2022;14. doi: ARTN 426. doi: 10.3390/pharmaceutics14020426

40. Collins HL, Adelman SJ, Butteiger DN, Bortz JD. Choline Supplementation Does Not Promote Atherosclerosis in CETP-Expressing Male Apolipoprotein E Knockout Mice. *Nutrients*. 2022;14. doi: 10.3390/nu14081651

41. Guo SH, Nighot M, Al-Sadi R, Alhmoud T, Nighot P, Ma TY. Lipopolysaccharide Regulation of Intestinal Tight Junction Permeability Is Mediated by TLR4 Signal Transduction Pathway Activation of FAK and MyD88. *J Immunol*. 2015;195:4999-5010. doi: 10.4049/jimmunol.1402598

42. Fang W, Xue H, Chen X, Chen K, Ling W. Supplementation with Sodium Butyrate Modulates the Composition of the Gut Microbiota and Ameliorates High-Fat Diet-Induced Obesity in Mice. *J Nutr*. 2019;149:747-754. doi: 10.1093/jn/nxy324

43. Tang G, Du Y, Guan H, Jia J, Zhu N, Shi Y, Rong S, Yuan W. Butyrate ameliorates skeletal muscle atrophy in diabetic nephropathy by enhancing gut barrier function and FFA2-mediated PI3K/Akt/mTOR signals. *Br J Pharmacol.* 2022;179:159-178. doi: 10.1111/bph.15693

44. Bach Knudsen KE, Laerke HN, Hedemann MS, Nielsen TS, Ingerslev AK, Gundelund Nielsen DS, Theil PK, Purup S, Hald S, Schioldan AG, et al. Impact of Diet-Modulated Butyrate Production on Intestinal Barrier Function and Inflammation. *Nutrients.* 2018;10. doi: 10.3390/nu10101499

45. Aguilar EC, Leonel AJ, Teixeira LG, Silva AR, Silva JF, Pelaez JM, Capettini LS, Lemos VS, Santos RA, Alvarez-Leite JI. Butyrate impairs atherogenesis by reducing plaque inflammation and vulnerability and decreasing NFkappaB activation. *Nutr Metab Cardiovasc Dis.* 2014;24:606-613. doi: 10.1016/j.numecd.2014.01.002

46. Bordoni L, Samulak JJ, Sawicka AK, Pelikant-Malecka I, Radulska A, Lewicki L, Kalinowski L, Gabbianelli R, Olek RA. Trimethylamine N-oxide and the reverse cholesterol transport in cardiovascular disease: a cross-sectional study. *Sci Rep.* 2020;10:18675. doi: 10.1038/s41598-020-75633-1

47. Richard C, Cristall L, Fleming E, Lewis ED, Ricupero M, Jacobs RL, Field CJ. Impact of Egg Consumption on Cardiovascular Risk Factors in Individuals with Type 2 Diabetes and at Risk for Developing Diabetes: A Systematic Review of Randomized Nutritional Intervention Studies. *Can J Diabetes.* 2017;41:453-463. doi: 10.1016/j.jcjd.2016.12.002

48. Shin JY, Xun P, Nakamura Y, He K. Egg consumption in relation to risk of cardiovascular disease and diabetes: a systematic review and meta-analysis. *Am J Clin Nutr.* 2013;98:146-159. doi: 10.3945/ajcn.112.051318

49. Meyer KA, Shea JW. Dietary Choline and Betaine and Risk of CVD: A Systematic Review and Meta-Analysis of Prospective Studies. *Nutrients.* 2017;9. doi: 10.3390/nu9070711

50. Nagata C, Wada K, Tamura T, Konishi K, Kawachi T, Tsuji M, Nakamura K. Choline and Betaine Intakes Are Not Associated with Cardiovascular Disease Mortality Risk in Japanese Men and Women. *J Nutr.* 2015;145:1787-1792. doi: 10.3945/jn.114.209296

SUPPLEMENT

Expanded methods

Plasma targeted metabolome

Plasma samples (20 μL per sample; n=10 per group) were prepared for quantitation of choline, betaine, TMA and TMAO level. The measurement was performed by BGI genomics (Shenzhen, Guang Zhou, China). In brief, plasma protein was precipitated by adding methanol/acetonitrile (15/85; 180 μL per sample). These plasma samples were then centrifuged (20,000 × g, 15 min, 4℃). The supernatants (10 μL per sample) were taken and mixed with pure acetonitrile (190 μL per sample). After the centrifugation (20,000 × g, 15 min, 4℃), the supernatants (5 μL per sample) were mixed with pure acetonitrile (55 μL per sample), and tested using liquid chromatography with tandem mass spectrometry (LC-MS/MS). Standard curve was prepared as follows. 1000 ppm (mg/mL) of each standard solution was prepared using methanol/acetonitrile (15:85), and then pure acetonitrile was used to gradually dilute standard solution to prepare a 0-200 ppb mixed standard into 9 standard concentration points. LC-MS/MS analysis was carried out using an ACQUITY UPLC I-Class (Waters, Framingham, MA, USA) coupled to QTRAP6500+ mass spectrometry (SCIEX, Framingham, MA, USA). Reversed-phase separation was performed on a BEH HILIC column (100 mm × 2.1 mm, 1.7 μm; Waters, Framingham, MA, USA) according to the manufacturer's instruction. The mobile phase consisted of ultrapure water, 0.15% formic acid, 10 mM ammonium formate and acetonitrile. Mass spectrometry was performed using ESI ion source in a positive ion mode. Using MultiQuant software (SCIEX, Framingham, MA, USA), the default parameters are used for automatic identification and integration of each multiple reaction monitoring (MRM) transition (ion pair), and manual inspection is assisted. The concentration of choline-related metabolites was obtained by substituting the integrated peak area of the targeted index in the sample into the standard curve, followed by multiplying by the dilution factor.

Metagenomics sequencing and analysis

Whole-genome shotgun sequencing of all samples (n=10 per group) was carried out on a DNBSEQ platform at BGI Genomics (Shenzhan, Guang Zhou, China). SOAPnuke was used to remove low quality sequences. Human sequences were removed using Bowtie2 [1]. The filtered high-quality reads were assembled into contigs using MEGAHIT [2], and only contigs of ≥ 300 bp were used. Genes were predicated by MetaGeneMark [3]. A non-redundant gene catalogue was constructed using CD-HIT [4]. Gene taxonomy was annotated to Kraken2 [5] database. High-quality reads were mapped back to the constructed non-redundant gene catalogue using Salmon [6] to calculate gene

abundance within each sample. Gene functional identification was annotated to Kyoto Encyclopedia of Genes and Genomes (KEGG) [7] and KEGG orthology (KO), and Carbohydrate-Active EnZymes (CAZy) [8]. Principal component analysis (PCA) [59] at the species level, linear discriminant analysis (LDAL) and relative abundance of pathways and enzymes were analysed using R packages.

Supplementary Table 1 List of primer sequences for the targeted mouse genes used in mRNA expression analysis

Gene	Forward primer (5'-3')	Reverse Primer (5'-3')
Abca1	CCCAGAGCAAAAAGCGACTC	GGTCATCATCACTTTGGTCCTTG
Abcg5	TGTCCTACAGCGTCAGCAACC	GGCCACTCTCGATGTACAAGG
Actb	AACCGTGAAAAGATGACCCAGAT	CACAGCCTGGATGGCTACGTA
Bsep	CTGCCAAGGATGCTAATGCA	CGATGGCTACCCTTTGCTTCT
CETP	CAGATCAGCCACTTGTCCAT	CAGCTGTGTGTTGATCTGGA
CutC	AGRGTTHGATYMTGGCTCAG	TGCTGCCTCCCGTAGGAGT
Cyp27a1	TCTGGCTACCTGCACTTCCT	CTGGATCTCTGGGCTCTTTG
Cyp7a1	CAGGGAGATGCTCTGTGTTCA	AGGCATACATCCCTTCCGTGA
Fmo1	AAACAAGCATAGCGGGTTTG	ATCCGGTTTTGCGTTGATAG
Fmo2	AGCTGTGGTCTTCGAGGATG	GGCAAGCTACACAAGCCTTT
Fmo3	GGAACTTGCACTTTGCCTTC	TAGGAGATTGGGCTTTGCAC
Fmo4	CGGAGCAGCTCATTAAAAGG	CTGAGTGAGCTCGTCCATGT
Fmo5	TGCCCTCACAAAGTGAAATG	GCTGGCTGTCCACATACCTT
Ldlr	GCATCAGCTTGGACAAGGTGT	GGGAACAGCCACCATTGTTG
Rplp0	GGACCCGAGAAGACCTCCTT	GCACATCACTCAGAATTTCAATGG
Srb-1	GTGCTGCTGGGGCTTGGAGG	CACTGGTGGGCTGTCCGCTG

Abca1, ATP-binding cassette subfamily A member 1; *Abcg5*, ATP-binding cassette transporter G member 5; *Actb*, β-actin; *ApoB*, apolipoprotein B; *Bsep*, bile salt export pump; *CETP*, CETP cholesteryl ester transfer protein; *CutC*, choline trimethylamine-lyase *Cyp27a1*, sterol 27-hydroxylase; *Cyp7a1*, cholesterol 7α-hydroxylase; *Fmo*, flavin monooxygenase; *Ldlr*, low density lipoprotein receptor; *Mttp*, microsomal triglyceride transfer protein; *Rplp0*, ribosomal protein lateral stalk subunit P0; *Srb-1*, scavenger receptor class B type 1.

REFERENCES

1. Langmead, B. and S.L. Salzberg, *Fast gapped-read alignment with Bowtie 2.* Nat Methods, 2012. **9**(4): p. 357-9.
2. Li, D., et al., *MEGAHIT: an ultra-fast single-node solution for large and complex metagenomics assembly via succinct de Bruijn graph.* Bioinformatics, 2015. **31**(10): p. 1674-6.
3. Zhu, W., A. Lomsadze, and M. Borodovsky, *Ab initio gene identification in metagenomic sequences.* Nucleic Acids Res, 2010. **38**(12): p. e132.
4. Fu, L., et al., *CD-HIT: accelerated for clustering the next-generation sequencing data.* Bioinformatics, 2012. **28**(23): p. 3150-2.
5. Wood, D.E., J. Lu, and B. Langmead, *Improved metagenomic analysis with Kraken 2.* Genome Biol, 2019. **20**(1): p. 257.
6. Patro, R., et al., *Salmon provides fast and bias-aware quantification of transcript expression.* Nat Methods, 2017. **14**(4): p. 417-419.
7. Kanehisa, M. and S. Goto, *KEGG: kyoto encyclopedia of genes and genomes.* Nucleic Acids Res, 2000. **28**(1): p. 27-30.
8. Lombard, V., et al., *The carbohydrate-active enzymes database (CAZy) in 2013.* Nucleic Acids Res, 2014. **42**(Database issue): p. D490-5.
9. Jolliffe, I.T. and J. Cadima, *Principal component analysis: a review and recent developments.* Philos Trans A Math Phys Eng Sci, 2016. **374**(2065): p. 20150202.

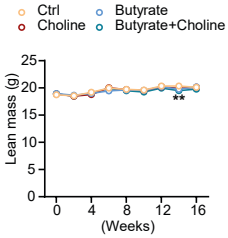

Fig. S1. Choline and butyrate have no effects on body lean mass in *APOE*3-Leiden.CETP* mice. Body lean mass was measured throughout the experimental period. Data are represented as mean±SEM (n=16-17 per group). Differences were assessed using one-way ANOVA followed by a Fisher's LSD post-test. ***P*<0.01, compared with the ctrl group.

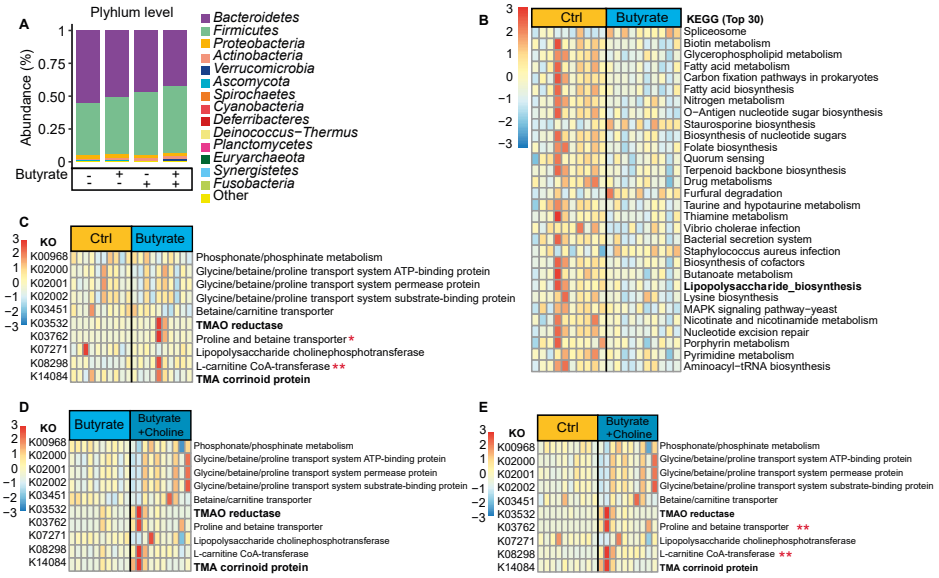

Fig. S2. Butyrate downregulates gut microbial genes involved in lipopolysaccharide biosynthesis in *APOE*3-Leiden.CETP* mice. At the end of the study, the cecal content was collected and sequenced using metagenomics (n=10 per group). (**A**) The abundance of top 15 microbial phyla. (**B**) Top 30 significantly regulated KEGG pathway between the ctrl and butyrate groups. (**C-E**) Relative changes of the gut microbial genes involved TMA metabolic pathway between groups. (**B-E**) Comparisons between groups were performed using Wilcoxon test. **P*<0.05; ***P*<0.01, compared with the ctrl group. KEGG, Kyoto Encyclopedia of Genes and Genomes; KO, KEGG Ortholog; TMA, trimethylamine; TMAO, trimethylamine N-oxide.

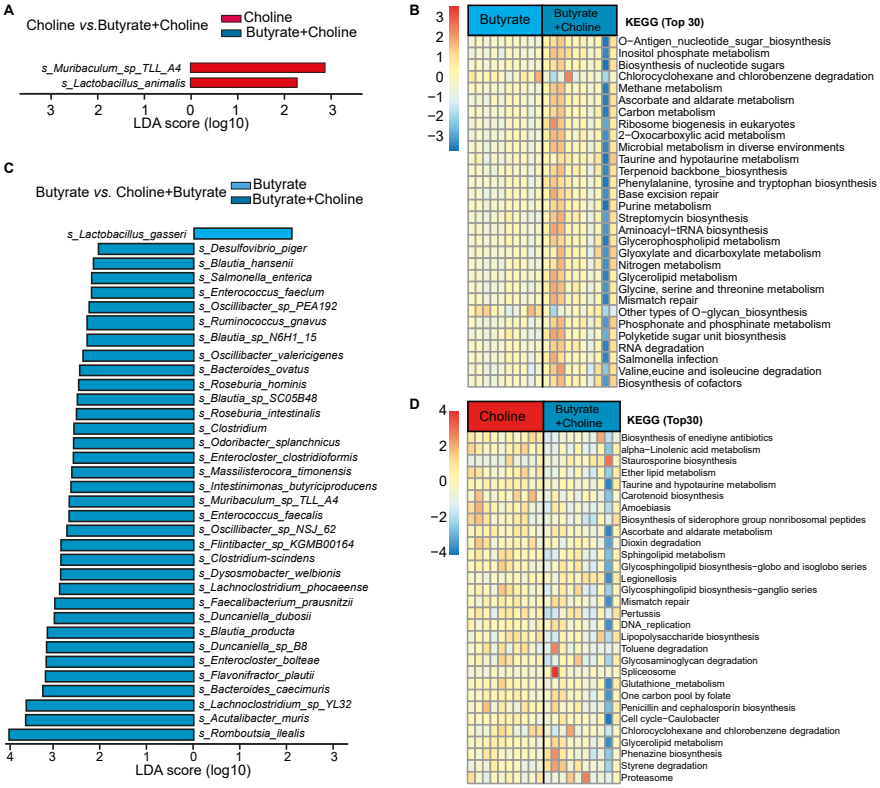

Fig. S3. Choline exerts greater effects on the gut microbial composition and function compared to butyrate in *APOE*3-Leiden.CETP* mice. (A and **C)** Linear discrimination analysis (LDA) effect size analysis was performed, and LDA scores calculated for differences in species-level abundance between groups. (**B** and **D**) Top 30 significantly regulated KEGG pathway between groups. (**B** and **D**) Comparisons between groups were performed using Wilcoxon test.

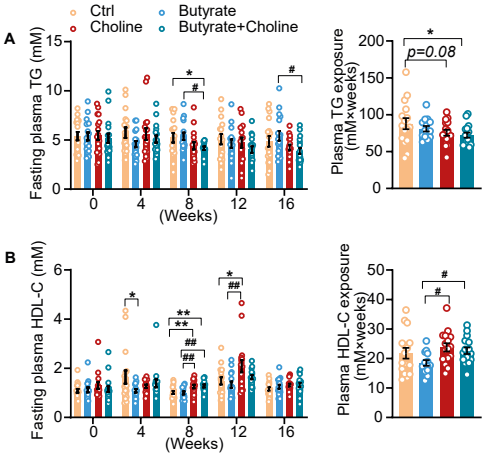

Fig. S4. Choline and butyrate do not evidently alter plasma lipid levels in *APOE*3-Leiden.CETP* mice. (A-B) Fasting plasma triglyceride (TG) and high-density lipoprotein cholesterol (HDL-C) levels were measured throughout the experimental period, and plasma TG and HDL exposure (mM x weeks) throughout the experimental period was calculated. Data are represented as mean±SEM (n=16-17 per group). Differences were assessed using one-way ANOVA followed by a Fisher's LSD post hoc test. **P*<0.05; ***P*<0.01, compared with the ctrl group; #*P*<0.05, ##*P*<0.01, compared to the butyrate group.

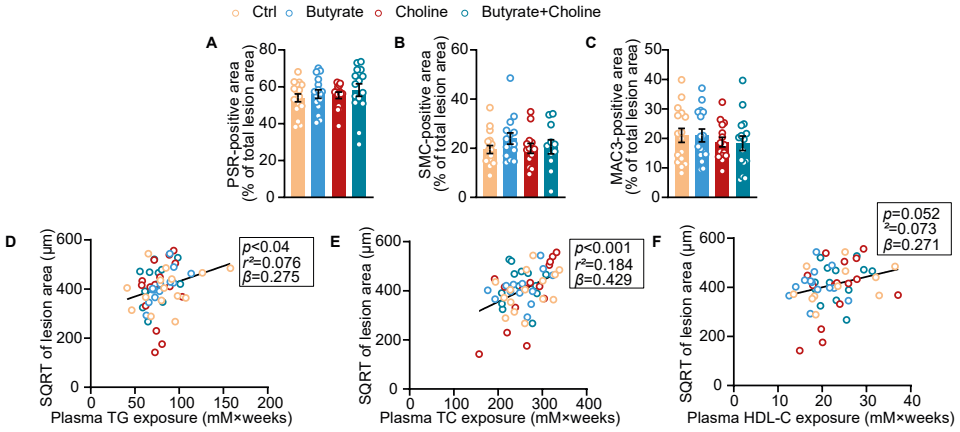

Fig. S5. Choline and butyrate have no impact on atherosclerotic lesion composition in *APOE*3-Leiden.CETP* mice. At the end of the study, atherosclerotic lesion composition was evaluated. To quantify the contents of collagen (**A**), smooth muscle cells (**B**) and macrophages (**C**) within the lesion, the valve area in the aortic root was stained with Picrosirius red (PSR), anti-α-smooth muscle cell actin (α-SMC actin) antibody and anti-MAC3 antibody, respectively. (**D-F**) The square root (SQRT) of the atherosclerotic lesion area was plotted against plasma TG exposure, total cholesterol (TC) exposure and HDL-C exposure during the 16-week treatment period, and linear regression analyses were performed. Data are represented as mean±SEM (n=13-16 per group). Differences were assessed using one-way ANOVA followed by a Fisher's LSD post hoc test.